JOURNAL OF OPTOELECTRONICS AND ADVANCED MATERIALS Vol. 12, No. 8, August 2010, p. 1652 - 1659

Design and fabrication of single mode polymer optical fiber gratings

W. WU[a], Y. LUO[a,b], X. CHENG[c], X. TIAN[a], W. QIU[c], B. ZHU[c], G.-D. PENG[b], Q. ZHANG[a*]
[a]*CAS Key Laboratory of Soft Matter Chemistry, Department of Polymer Science and Engineering, University of Science and Technology of China, Anhui Key Laboratory of Optoelectronic Science and Technology, Hefei, Anhui 230026, P.R.C.*
[b]*School of Electrical Engineering and Telecommunications, University of New South Wales, Sydney, 2052, Australia*
[c]*Anhui Key Laboratory of Optoelectronic Science and Technology, Key Laboratory of Quantum Information, Department of Electronic Engineering and Information Science, University of Science and Technology of China, Hefei, Anhui 230026, P.R.C.*

The design of single mode polymer optical fiber (POF) gratings was reported, combined by the Bragg condition, weakly guiding condition, single mode condition and the experimental conditions. In the following, the reflection spectrum of benzildimethylketal (BDK) doping POF gratings was simulated theoretically. Then photosensitive single mode POF doped with BDK was fabricated using Teflon technique, with the cladding of the copolymer of methyl methacrylate (MMA)-ethyl methacrylate (EMA) (60/40 v%) and the core of the copolymer of MMA-EMA-benzyl methacrylate (BzMA) (50/45/3 v%) doped with BDK (2 v%). At last, POF gratings were written in such a single mode photosensitive POF doped with BDK, whose Bragg wavelength is around 1572 nm, reflection intensity is about 7 dB, and the full width at half maximum is about 0.15 nm.

(Received June 11, 2010; accepted August 12, 2010)

Keywords: Photosensitive polymer optical fiber, Sinlge mode polymer optical fiber, Polymer optical fiber gratings, Benzildimethylketal

1. Introduction

POFs have received increasing attention not only for their clear technical advantages over silica fibers, such as flexibility and a large core diameter, which enables efficient connection and coupling resulting in a low-cost system for a local area network, but also for its excellent compatibility of base polymer material with many functional organics, such as luminescent dye, azo dye, rare earth complex and so on.[1-5] Special functional POFs are being developed for various active and passive photonic devices. Importantly from our perspective, special functional dopants can be introduced into the base polymer matrix of POF for enhancing photosensitivity and making POF gratings.[4,6-9]

Since gratings fabricated in POF in the past decade[1], they have received a lot of attentions due to their special mechanical properties, such as favourable strain transfer coefficient with texiles, high strain resolution, wide dynamic range and flexibility,[10-14] thermal properties, such as large thermo-optic coefficient and large thermal expansion coefficient,[15] and chemical properties, such as good biocompatibility and high moisture absorption.[16,17] They have found a wide range of applications, such as a bend sensor, a strain sensor, a tunable laser with wide dynamic range, and other optical fiber devices.[12,15,18-22] So a lot of work has been done related with POF gratings.[1,10-13,15-18,20-22] So far, although there are many reports about POF design and fabrication,[7,23-26] the design of POF gratings is still rare. So it is very essential and important for the fabrication of POF gratings.

It is known that the innate photosensitivity of PMMA after irradiation with UV light at 325 nm or 365 nm has been discovered for more than 30 years by Tomlinson *et al.*,[27] but the photosensitivity was too weak to make POF gratings with good performance and high strength because of the high power and long UV irradiation time.[6,20] Therefore, different materials, such as azo dye, trans-4-stilbenemethanol and methyl vinyl ketone were doped into the core of POFs to enhance the photosensitivity of PMMA and fabricating high photosensitive POFs.[4,6,7] Meanwhile in order to have a high reflectivity and to be compatible with other photonic devices, a single mode POF is preferability condition for fabricating POF gratings.[7] Take these factors into account, in this paper, firstly we design the photosensitive POF used for POF gratings in theory. And the reflection spectrum of such POF gratings is simulated and the influence factors upon the reflectivity are investigated further. Then using Teflon technique, single mode POF doped with BDK, which is a classic photosensitive dye

that exhibits photodegradation into two radicals by an α-splitting under a very wide band of UV illumination,[28] is fabricated. Finally, a modified sagnac interferometeric technique is used to fabricate POF gratings in such a photosensitive POF.

2. Design of POF gratings

2.1 Composition and diameter of PMMA based POF

To fabricate the POF gratings, first of all, PMMA based POF should be made. In our work, the POF was drawn from the POF preform. In making a polymer fiber preform, the tuning and controlling of the refractive index are important. In our case, the difference between the refractive indices of the core and cladding is controlled by adding BzMA or EMA to the core and cladding. The index varies with the amount of them. Before the polymerization of POF preform, the monomers and the ratio of them should be assured. It often has four kinds of materials used for the fiber core. In our work, MMA, EMA, BzMA and BDK are mixed to be polymerized as the core materials, in which PMMA is the base material, EMA and BzMA are used to tuning the refractive index, and BDK is used as the photosensitive material.

As we all know, the refractive index of a compound can be estimated from its molar refraction and molecular volume according to the Lorentz-Lorenz equation,[29]

$$\frac{n^2-1}{n^2+2}=\frac{[R]}{V}\equiv\phi, \tag{1}$$

$$n=\sqrt{(2\phi+1)/(1-\phi)}, \tag{2}$$

where n is the refractive index, $[R]$ is molar refraction, V is the molecular volume, and ϕ is the molar refraction per unit volume. So the refractive index of the fiber core (n_{co}) can be given by

$$\phi_{co}=\sum_{i=1}^{4}c_i\frac{n_i^2-1}{n_i^2+2} \tag{3}$$

$$n_{co}=\sqrt{(2\phi_{co}+1)/(1-\phi_{co})} \tag{4}$$

where c_i is the volume fraction of unit i in the fiber materials and $\sum_{i=1}^{4}c_i=1$, in which i = 1 stands for PMMA, i = 2 for PEMA, i = 3 for PBzMA and i = 4 for BDK, and their refractive indices at 1550 nm are listed in Table 1. Although it would obtain higher refractive index change, due to higher loss of POF doped with more BDK in the fiber core, c_4 should not be too high. In our work, c_4 = 2 % as listed in Table 2.

Table 1. Experiment conditions.

Materials	PMMA	PEMA	PBzMA	BDK
Refractive index(RI)[a]	1.4793	1.4729	1.5468	1.5821
Writing setup	Phase mask 1	1061.4 nm designated for 248 nm writing light Suitable for the modified sagnac interferometeric method		
	Phase mask 2	1033.56 nm designated for 355 nm writing light Suitable for the simple phase mask method		
	Writing light source 1	355nm frequency-tripled Nd:YAG pulse laser (10 Hz, 6 ns pulse width)		
	Writing light source 2	A semiconductor-pumped Nd:YAG laser with output at 355 nm		
Monitoring setup	ASE	Thorlabs ASE-FL7002 (1530~1610 nm)		
	Tunable laser	ANDO AQ4321D (1520~1620 nm)		
	OSA	Agilent AQ 4317C OSA		
		Agilent 86140B OSA		

[a]The RI value was detected at 1550 nm by SPA 4000 from Sairontech Company.

Only two kinds of materials are used for the fiber cladding, which is the copolymer of EMA and MMA. Similarly, the refractive index of the fiber cladding (n_{cl}) can be given by

$$\phi_{cl}=c_1\frac{n_1^2-1}{n_1^2+2}+c_2\frac{n_2^2-1}{n_2^2+2} \tag{5}$$

$$n_{cl}=\sqrt{(2\phi_{cl}+1)/(1-\phi_{cl})} \tag{6}$$

where $c_1+c_2=1$. By just tuning c_2, the refractive index of the cladding material can be adjusted.

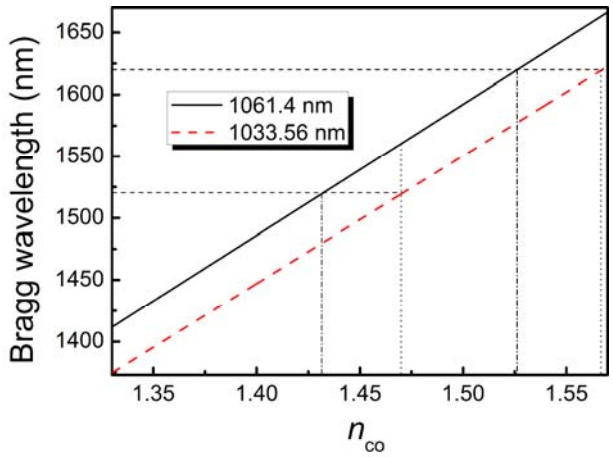

Fig. 1. The relationship between the Bragg wavelength and the refractive index of fiber core needed.

In addition, there is a famous Bragg condition in the single-mode fiber grating, which provides the simple and yet very important relation among the Bragg wavelength (λ_B), the effective refractive index (n_{eff}) of optical fiber and the grating period Λ of the index variation (Δn) and is given by

$$\lambda_B = 2n_{eff}\Lambda \tag{7}$$

As n_{eff} is often slightly less than the refractive index of the fiber core, it is usually replaced by the later and there will be

$$n_{co} \approx n_{eff} \tag{8}$$

and

$$\lambda_B = 2n_{co}\Lambda \tag{9}$$

which shows that the Bragg wavelength changes linearly with the refractive index of fiber core. By tuning the composition of fiber core materials, the refractive index of the fiber core can be changed as Eqs. (3) and (4) described, so can the Bragg wavelength for certain grating period (often decided by the phase mask we obtained). In the present condition, only two phase masks listed in Table 1 can be used, with grating period of 1061.4 and 1033.56 nm. Meanwhile, the monitoring system we have as listed in Table 1 can only detect gratings with its Bragg wavelength from 1520 to 1620 nm. So using our present experimental conditions to write and monitor FBGs in POF, we need to tune the composition of the fiber core materials to get a suitable refractive index as shown in Figure 1. It shows that the refractive index of fiber core materials could be varied from 1.471 to 1.523 (around 1550 nm).

As mentioned above, when c_4 = 2 % at different concentration (c_1) of PMMA, we can change the composition of BzMA and EMA to make sure that the refractive index of the fiber core is between 1.471 to 1.523 as shown in Figure 2. In our work, as the POF is mostly based on PMMA, so c_1 must be larger than 50 %. Seen from Figure 2, c_3 must be less than 48 %, if we want to control the refractive index of the fiber core between 1.471 and 1.523. And it is found that with the c_1 increasing, the maximum value of c_3 would be reduced. Especially in our work, c_1 and c_4 are about 50 % and 2 %, respectively. So when c_3 is less than 48 %, the refractive index of the fiber core could be controlled to satisfy the experiment conditions through tuning the composition of BzMA and EMA. In our work, c_3 = 3 % was chosen so c_2 = 45 % as listed in Table 2. And n_{co} could be deduced according to Eqs. (3) and (4), which is about 1.4804 in theory.

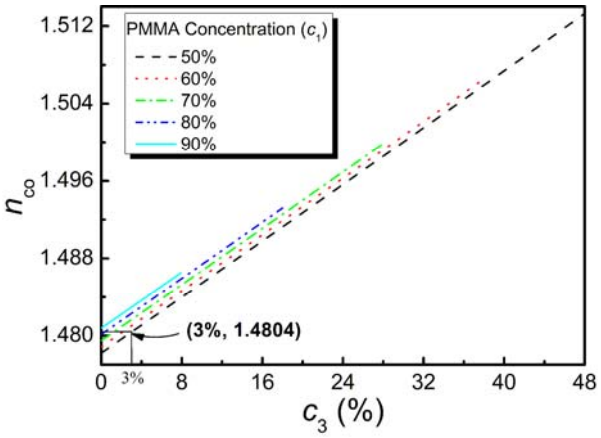

Fig. 2. The relationship between the refractive index of the fiber core and c_3 with different PMMA concentration.

Ordinarily for the weakly guidance condition of a single mode optical fiber, the relative difference of n_{co} and n_{cl} ($\Delta = \frac{n_{co}^2 - n_{cl}^2}{2n_{co}^2}$) could be simplified as $\Delta \approx \frac{n_{co} - n_{cl}}{n_{co}}$, when $0.001 < \Delta < 0.01$, which means that a very small Δ can constitute a good optical waveguide structure.[30,31] So $0.99n_{co} < n_{cl} < n_{co}$, which could be easily satisfied by tuning the ratio of MMA and EMA. After the composition of fiber core materials is decided as listed in Table 2, there is $1.4656 < n_{cl} < 1.4804$. By tuning the composition of MMA and EMA, the refractive index of the cladding could satisfy the requirement. In our work, for the cladding c_1 and c_2 are 60 % and 40 % as listed in Table 2, respectively. So the refractive index of the fiber cladding is about 1.4767 according to Eqs. (5) and (6).

In addition, in order to have a high reflectivity and to be compatible with other photonic devices, a single mode POF is required for fabricating POF gratings. The mode number is related with several parameters of the POF, and the normalized frequency should obey the following equation:[30]

$$V = \frac{2\pi}{\lambda} \cdot a\sqrt{n_{co}^2 - n_{cl}^2} < 2.4 \tag{10}$$

where $2a$ and λ are the diameters of fiber core and working wavelength of POF gratings, respectively. So the

diameter of the POF core should be controlled in terms of the difference of n_{co} and n_{cl}. Especially, the smaller the difference, the larger the fiber core and the easier the fabrication. When POF gratings are working from 1520 to 1620 nm, according to Eq. (10), there will be $2a < 11.3$ μm ($\lambda = 1.55$ μm) in theory, which means that the diameter of the fiber core should be controlled less than 11.3 μm. Besides of the refractive index, mechanical and thermal properties of polymer can also be changed. Meanwhile, we can modify the mechanical and thermal properties, according to specific application by the choice of the initiators and chain transfer agents.[32]

2.2 The reflection spectrum in theory

For a single-mode Bragg reflection grating with sinusoidal index change along the fiber axis, the coupling coefficient is given by[33]

$$\kappa = \frac{\pi \Delta n}{\lambda} \tag{11}$$

where λ is the light wavelength and Δn is the index variation in the fiber core.

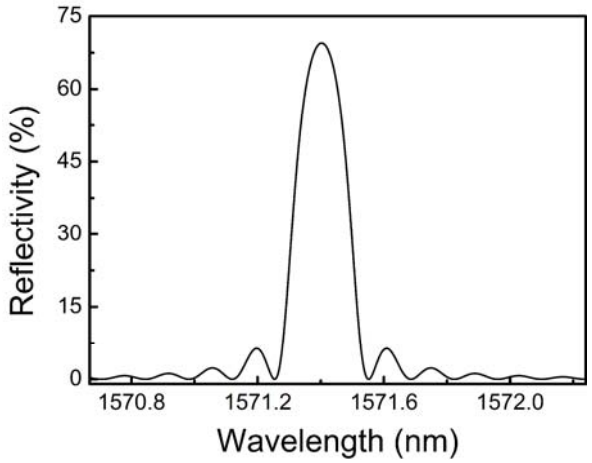

Fig. 3. The simulated reflection spectrum of POF gratings.

The power reflection coefficients R from a fiber Bragg grating can be worked out as follows [30,33]

$$R = \frac{\kappa^2 \sinh^2(qL)}{\delta^2 \sinh^2(qL) + q^2 \cosh^2(qL)} \tag{12}$$

where L is the length of the Bragg gratings, δ is the difference between the actual propagation constant β ($\beta = \frac{2\pi}{\lambda} n_{\text{eff}}$) and the propagation constant at Bragg wavelength β_B ($\beta_B = \frac{2\pi}{\lambda} n_{\text{eff}}$) and $q^2 = \delta^2 - \kappa^2 > 0$. Figure 3 shows the calculated reflection spectrum of the Bragg grating with sinusoidal modulation index (Δn) of 1.0×10^{-4} and grating length of 6 mm. The period of the gratings is about 530.7 nm half of the phase mask 1. The effective refractive index of the fiber core is about 1.4804. The reflection reaches a maximum of 69.5 % at 1571.4 nm with a full width at half maximum(FWHM) of 0.18 nm. The sidelobes of the maximum peak are due to multiple reflections to and from opposite ends of the grating region.

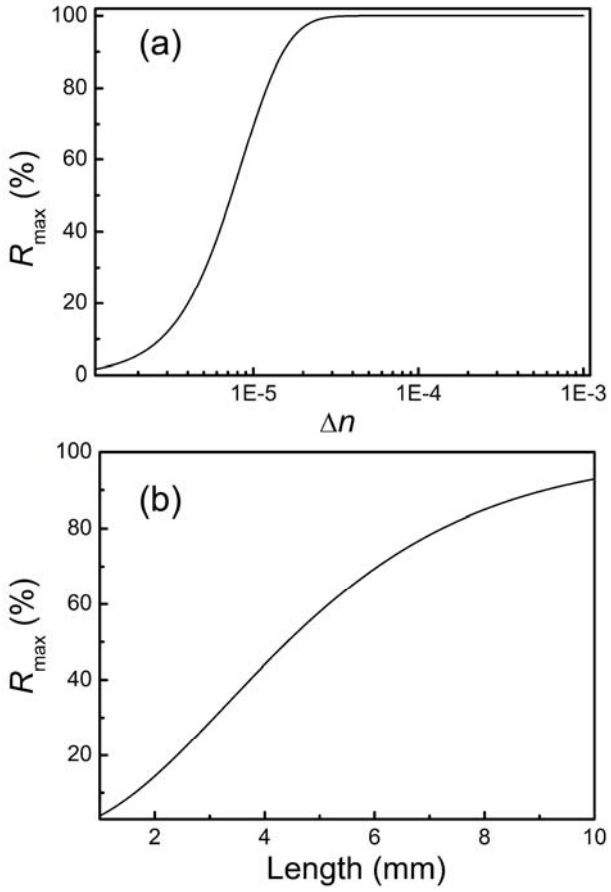

Fig. 4. (a) The maximum reflectivity as a function of the refractive index variation when the grating length is 6mm and Bragg wavelength is 1571.4 nm. (b) The maximum reflectivity as a function of the grating length when refractive index variation is 1.0×10^{-4} and Bragg wavelength is 1571.4 nm.

As a simple example, we consider the case when the frequency offset is $\delta = 0$, i.e. the incident wavelength is at the center of the band-gap, where the maximum reflectivity R_{max} happens. A simple expression for R_{max} is obtained as [33]

$$R_{\max} = \tanh^2(\kappa L) \tag{13}$$

It is obvious that the maximum reflectivity increases with the increase of both the refractive index variation Δn and grating length L as shown in Figure 4. Seen from

Figure 4 (a), when the grating length is 6 mm and Bragg wavelength is 1571.4 nm, the maximum reflectivity increases with the increase of the refractive index variation, till the refractive index variation reaches 2.5×10^{-5}. And then it reaches a saturated value of almost 100 %. Seen from Figure 4 (b), when the refractive index variation is 1.0×10^{-4} and Bragg wavelength is 1571.4 nm, the maximum reflectivity increases steadily with the increase of the grating length.

For the designed POF gratings, the refractive index variation will change with time illumination. According to Ref.[34], for certain light intensity the refractive index change of BDK doping PMMA has the following function:

$$\Delta n = a\sqrt{t} - b \tag{14}$$

where a and b are the constants fitted to the experimental data as reported in Ref.[34], in which a is about 1.67×10^{-4}. Combining Eqs. (11) and (12) with (13), the maximum reflectivity after t mins illumination is as follows:

$$R_{\max} = \tanh^2\left[\frac{\pi L(a\sqrt{t} - b)}{\lambda_B}\right] \tag{15}$$

If the refractive index of POF doped BDK varies as the same described in Ref.[34], the maximum reflectivity changes after t min UV illumination as shown in Fig. 5. Seen from Fig. 5, for different b value the $R_{\max}$ has a different minimum value point. The value increases fast and reaches a saturated value, which means that the $R_{\max}$ can not increase unrestrictedly. It also indicates that the refractive index variation of POF doped with BDK would reach a maximum value in a short time, especially for the strong light source used compared with that of Ref. [34].

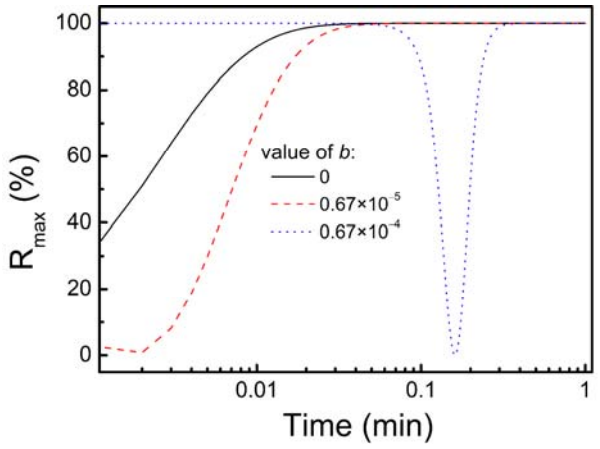

Fig. 5. The maximum reflectivity as a function of illumination time with different b when the grating length is 6 mm and Bragg wavelength is 1571.4 nm.

3. Photosensitive POF fabrication

To obtaining photosensitive POF, BDK was doped into the fiber core when polymerizing it by Teflon technique, in which BDK is activated by a transition within the molecular orbits of the >C=O group followed by an α-splitting to produce free radicals irradiated by UV light inducing refractive index change. [28,34] The fabrication process is illustrated in Scheme 1. First, using Teflon technique a hollow stick was made by the copolymer of MMA and EMA according to the procedure reported before. [7,32] In our work, the inner diameter of the glass tube is about 18 mm and the diameter of the Teflon line is about 0.8 mm. Then, the mixture solution of MMA, EMA and BzMA (volume ratio = 50:45:3), 0.1076 g BDK, 0.0144 g lauryl peroxide as an initiator, 0.0133 g *n*-butyl mercaptan as a chain-transfer agent, were mixed in a vessel. Under the minus pressure, the above solution was filled into the hollow stick as a core material. And then the stick was put into an oven and the thermal polymerization was carried out in it. The temperature was increased gradually from 36 ºC to 88 ºC in 4.5 days until solidification was fulfilled.

Table 2 . Fiber parameters and grating fabrication conditions.

POF Specification	Grating Formation Process
Cladding (MMA:EMA = 60:40 v%) core (MMA:EMA:BzMA:BDK = 50:45:3:2 v%) n_{co}-n_{cl}: ~ 0.001(measured), 0.0037(calculated) n_{cl}: ~ 250.2 μm n_{co}: ~ 17.6 μm	355 nm frequency-tripled Nd:YAG pulse laser frequency: 10 Hz pulse width: 6 ns average power intensity: 81mW/cm^2 grating length: 6 mm

Then the refractive index profile of the POF perform is detected and the refractive index difference between the core and the cladding is about 0.001 (633 nm), which is smaller than the designed value 0.0037 in theory. In addition, the preform core diameter is about 1.2 mm, which is larger than the diameter of the Teflon line. All these deviations with our design are attributed to the diffusion and dissolution in the interfacial-gel polymerization.[35] According to these actual values (n_{co} = 1.4804, $n_{co} - n_{cl}$ = 0.001 and λ = 1.55 μm) and Eq. (10), the fiber core diameter should be less than 21.7 μm. So it requires that the fiber diameter of the POF should be less than 326 μm. Then the preform was heat-drawn into an optical fiber at 225 ºC by a taking up spool. By tuning the drawing velocity, POF with different diameter could be made. In our work, the overall diameter of the POF doped with BDK is about 250.2 μm with the core diameter of about 17.6 μm as listed in Table 1.

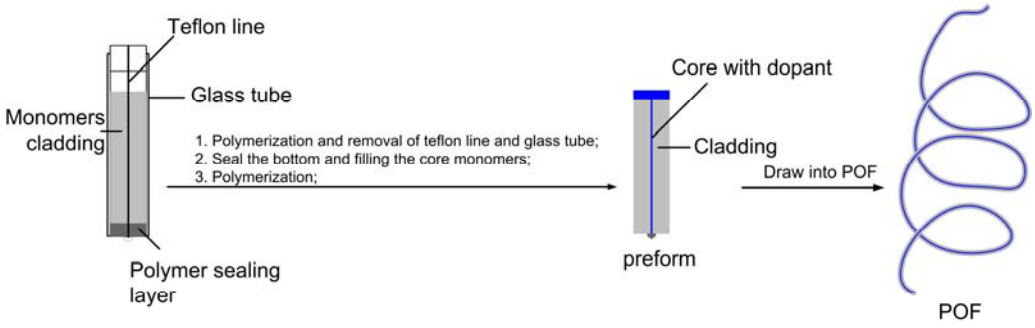

Scheme 1. The diagram of the processes in the POF fabrication using Teflon technique.

4. POF gratings fabrication

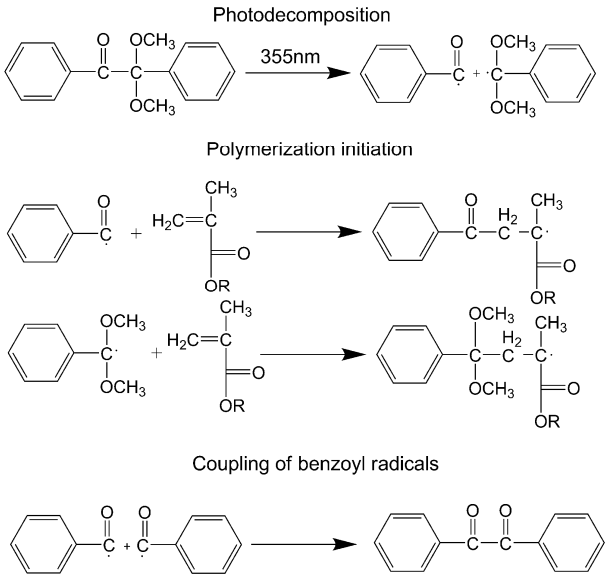

Scheme 2. Possible photochemical reactions of BDK in POF.

As mentioned above, the POF has a photosensitive core doped with BDK, which is activated by a transition within the molecular orbits of the >C=O group followed by an α-splitting to produce free radicals irradiated by UV light (Scheme 2). Then, a series of reactions could happen in the following, including the polymerization of rudimental monomers, the photolock of high index ketal fragments and so on.[28,34] All these reactions would be the factors inducing refractive index change in POF.

According to our condition, two kinds of writing techniques as shown in Scheme 3 could be used to inscribe the POF gratings. One is the modified sagnac interferometeric method, the other is the simple phase mask method. The difference between them is that the latter needs a phase mask designated for the writing light, as the period is independent of the irradiating UV wavelength.[36]

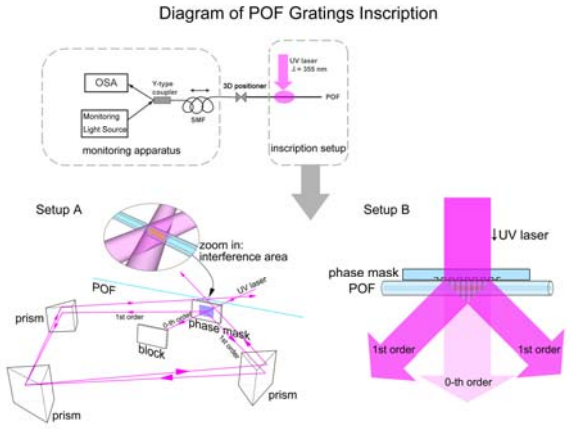

Scheme 3. The diagram of POF gratings inscription with the modified sagnac interferometeric system (Setup A) and the simple phase mask system (Setup B).

For a phase mask with a period of 1.0614 μm designed for 248 nm operation(but it is easily damage POF, so 248nm laser would not be chosen as the writing light source for POF gratings fabrication), to overcome the effects of the zero-order diffraction on the grating writing in optical fibers, the modified sagnac interferometeric method was chosen to inscribe POF gratings with a 355 nm frequency-tripled Nd:YAG pulse laser as shown in Scheme 3 A. Seen from Scheme 3A, it can be seen that POF is placed on the top of the phase mask. Three reflective prisms were aligned so that the counter-propagating coherence beams will be directed to the fiber core for writing grating.

For a phase mask with a period of 1.033.56 nm designed for 355 nm operation, the setup for writing fiber gratings by the simple phase mask method is very simple: just placing the optical fiber almost in contact with the

corrugations of the phase mask, as shown in Scheme 3B. The UV light, which is incident normal to the phase mask, passes through and is diffracted by the corrugations of the phase mask. The profile of the phase mask is designed so that the zero order of the diffractive beam is suppressed to less than 1 % of the transmitted power by controlling the depth of the corrugations in the phase mask. Therefore, the diffractive +1 and −1 order will be maximized. Thus, the two ±1 diffractive order beams interfere to form the fringe pattern that photoimprints a refractive index modulation in the fiber core. The period of photoimprinted gratings in the fiber core is half of the period of the phase mask gratings. Therefore, the period is independent of the irradiating UV wavelength.

Besides, in order to monitor the grating formation, monitoring light coming from ASE (Thorlabs ASE-FL7002) or Tunable laser (AQ 4321D of ANDO) is launched into POF through a silica fiber coupler. On reaching the grating, portion of the light will be reflected while the rest will propagate through the grating and down the fiber. An optical spectrum analyzer (Agilent 86140B OSA or AQ 4317C OSA) is used to detect the reflection and determine the reflection spectrum of the grating. Grating formation parameters are described in Table 2. The UV laser beam is not focused and has an effective spot size of 6 mm, so the length of the grating is considered to be about 6 mm.

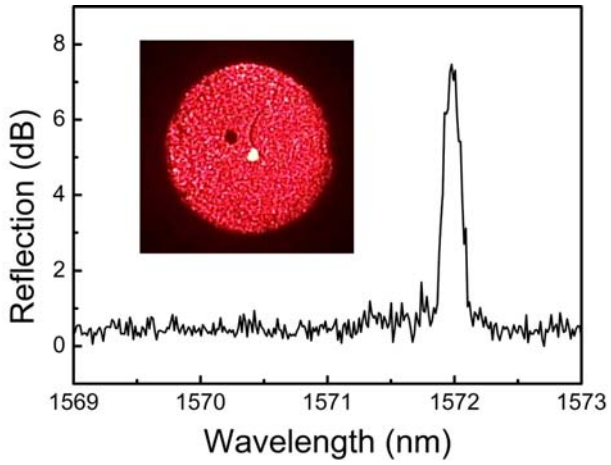

Fig. 6. The reflection spectrum of FBGs in POF doped with BDK after 7 mins 355 nm UV exposure. The inset is the near field pattern of such POF at 650 nm.

In this work, the modified sagnac interferometeric technique was used to write BDK doping POF gratings. According to Eq. (13), the normalized frequency of the POF at 1570 nm is about 1.9 smaller than 2.4.[30] Hence, single mode is expected as shown in Figure 6. After 7 mins 81 mW/cm^2 355 nm illumination, the reflection spectrum of FBGs formed as shown in Figure 6. Seen from the near-field pattern of the POF fiber shown in the inset of Figure 6, there is a hole in the cladding which is coming from the bubbles when drawing. The Bragg wavelength is around 1572 nm, the reflection intensity is about 7 dB, and FWHM is about 0.15 nm. According to Eq. (9), the core refractive index at 1572 nm could be deduced about 1.4810, which is very close to the designed value (1.4804), but still larger than the designed value. The reason for this may be attributed to the high sensitivity of the Bragg wavelength to the surrounding temperature and strain.[15] Besides, the reflection intensity is lower compared with the simulated result which may be attributed to long time illumination for the damage of gratings at the later time,[9] which means that we need use lower writing power and shorter writing time in future.

In addition, the working Bragg wavelength is 1572 nm, which is indeed not the most desirable, but it remains the most successful demonstrated operation wavelength for POF FBGs. Especially it is compatible with existing silica FBG systems and hence being investigated for various applications in the 1550 nm regions.[12,18,20,37] But by just changing another phase mask and suitable monitoring system, POF gratings at the optical window of POF, i.e. at 600~700 nm could be fabricated in POF doped with BDK in future.

5. Conclusions

Combining the Bragg condition, weakly guiding condition and single mode condition with our experimental conditions, POF gratings are designed and their reflection spectrum is simulated in theory. The results show that the refractive index of fiber core materials could only be varied from 1.471 to 1.523 and the diameter of the fiber core should be controlled less than 11.3μm in theory. And it is found that the maximum reflectivity is increased with the increase of both the refractive index variation and grating length. Especially for the POF doped with BDK, the maximum reflectivity has a novel growth with the illumination time in theory, and the refractive index variation could reach the maximum value in a short time. Then POF doped with BDK was fabricated using Teflon technique, with the cladding of the copolymer of MMA-EMA (60/40 v%) and the core of the copolymer of MMA-EMA-BzMA (50/45/3 v%) doped with BDK (2 v%). The fiber optical diameter is about 250.2 μm and the fiber core diameter is about 17.6 μm. Finally, using the modified sagnac interferometeric technique, the POF gratings is inscribed in POF doped with BDK, whose Bragg wavelength is around 1572 nm, reflection intensity is about 7 dB, and FWHM is about 0.15 nm, which could be used for the measurement of refractive index, strain, temperature, etc. in future.

Acknowledgements

This research is supported by National Natural Science Foundation of China (No. 50773075, 50703038

and 50973101), Chinese Academy of Sciences (kjcx3.sywH02 and kjcx2-yw-m11), and National Basic Research Program of China (No. 2006cb302900).

Reference

[1] G. D. Peng; X. Xiong; P. L. Chu, Opt. Fiber Technol. **5**, 242 (1999)
[2] K. Kuriki; Y. Koike; Y. Okamoto, Chem. Rev. **102**, 2347 (2002)
[3] H. Liang; Q. J. Zhang; Z. Q. Zheng; H. Ming; Z. C. Li; J. Xu; B. Chen; H. Zhao, Opt. Lett. **29**, 477 (2004)
[4] Y. H. Luo; J. L. Zhou; Q. Yan; W. Su; Z. C. Li; Q. J. Zhang; J. T. Huang; K. Y. Wang, Appl. Phys. Lett. 91(2007)
[5] A. Argyros. Kiriama Pty. Ltd.: 2009.
[6] J. M. Yu; X. M. Tao; H. Y. Tam, Opt. Lett. **29**, 156 (2004)
[7] Z. Li; H. Ma; Q. Zhang; H. Ming, J. Optoelectron. Adv. Mater. **7**, 1039 (2005)
[8] Z. C. Li; H. Y. Tam; L. X. Xu; Q. J. Zhang, Opt. Lett. **30**, 1117 (2005)
[9] Y. H. Luo; Q. J. Zhang; H. Y. Liu; G. D. Peng, Opt. Lett. **35**, 751 (2010)
[10] Z. Xiong; G. D. Peng; B. Wu; P. L. Chu, IEEE Photonics Technol. Lett. **11**, 352 (1999)
[11] G. D. Peng; P. L. Chu. Optical Information Processing Technology, 303 (2002)
[12] X. Chen; C. Zhang; D. J. Webb; R. Suo; G. D. Peng; K. Kalli. 20th International Conference on Optical Fibre Sensors, 750327 (2009)
[13] K. S. C. Kuang; S. T. Quek; C. G. Koh; W. J. Cantwell; P. J. Scully, J. Sensors 2009, 13 (2009)
[14] C. C. Ye; J. M. Dulleu-Barton; D. J. Webb; C. Zhang; G. D. Peng; A. R. Chambers; F. J. Lennard; D. D. Eastop. 20th International Conference on Optical Fibre Sensors, 12020 (2009)
[15] H. B. Liu; H. Y. Liu; G. D. Peng; P. L. Chu, Opt. Commun. **219**, 139 (2003)
[16] D. J. Webb; H. Dobb; M. Aressy; S. Kukureka; A. Argyros; M. Large; J. Barton; A. Fender; J. Jones; W. MacPherson; M. S. Lopez; K. Kalli; G. D. Peng. the 14th International Conference on Polymer Optical Fiber, 325 (2005)
[17] D. J. Webb; K. Kalli; C. Zhang; I. Johnson; X. F. Chen; S. R. David; D. B. Janice; C. Ye; G. D. Peng; A. Argyros; M. C. J. Large. The 18th International Conference on Plastic Optical Fibers 4(2009)
[18] H. Y. Liu; H. B. Liu; G. D. Peng; P. L. Chu, Opt. Commun. **266**, 132 (2006)
[19] D. J. Webb; K. Kalli; C. Zhang; M. Komodromos; A. Argyros; M. Large; G. Emiliyanov; O. Bang; E. Kjaer. Photonic Crystal Fibers II, L9900 (2008)
[20] C. Zhang; K. Carroll; D. J. Webb; I. Bennion; K. Kalli; G. Emiliyanov; O. Bang; E. Kjaer; G. D. Peng. 19th International Conference on Optical Fibre Sensors, G44 (2008)
[21] C. Zhang; X. Chen; D. J. Webb; G. D. Peng. 20th International Conference on Optical Fibre Sensors, 750380 (2009)
[22] I. P. Johnson; D. J. Webb; K. Kalli; M. C. J. Large; A. Argyros. Photonic Crystal Fibers IV, 77140D (2010)
[23] M. A. van Eijkelenborg; M. C. J. Large; A. Argyros; J. Zagari; S. Manos; N. A. Issa; I. Bassett; S. Fleming; R. C. McPhedran; C. M. de Sterke; N. A. P. Nicorovici, Opt. Express **9**, 319 (2001)
[24] Y. N. Zhang; K. Li; L. L. Wang; L. Y. Ren; W. Zhao; R. C. Miao; M. C. J. Large; M. A. van Eijkelenborg, Opt. Express **14**, 5541 (2006)
[25] W. X. Wu; J. Xu; Y. H. Luo; J. W. Yang; H. Ming; B. Chen; Q. J. Zhang, J. Appl. Polym. Sci. **111**, 730 (2009)
[26] A. Yeung; P. L. Chu; G. D. Peng; K. S. Chiang; Q. Liu, J. Lightwave Technol. **27**, 101 (2009)
[27] W. J. Tomlinson; I. P. Kaminow; E. A. Chandross; R. L. Fork; W. T. Silfvast, Appl. Phys. Lett. **16**, 486 (1970)
[28] O. H. Park; J. I. Jung; B. S. Bae, J. Mater. Res. **16**, 2143 (2001)
[29] N. Tanio; M. Irie, Jpn. J. Appl. Phys. Part 1 - Regul. Pap. Short Notes Rev. Pap. **33**, 3942 (1994)
[30] H. Ming; G. Zhang; J. Xie, Optoelectronic Technology, Publishing company of USTC, Hefei, (1998)
[31] V. Singh; B. Prasad; S. P. Ojha, Microw. Opt. Technol. Lett. **46**, 271 (2005)
[32] G. D. Peng; P. L. Chu; Z. J. Xiong; T. W. Whitbread; R. P. Chaplin, J. Lightwave Technol. **14**, 2215 (1996)
[33] A. Ankiewicz; Z. H. Wang; G. D. Peng, Opt. Commun. **156**, 27 (1998)
[34] H. Franke, Appl. Opt. **23**, 2729 (1984)
[35] Q. J. Zhang; P. Wang; Y. Zhai, Macromolecules **30**, 7874 (1997)
[36] H. Liu, Polymer Optical fiber Bragg Gratings, University of New South Wales, (2003)
[37] H. Dobb; K. Carroll; D. J. Webb; K. Kalli; M. Komodromos; C. Themistos; G. D. Peng; A. Argyros; M. C. J. Large; M. A. van Eijkelenborg; Q. Fang; I. W. Boyd. Optical Sensing II, 618901 (2006)

*Corresponding author: yhluo3@mail.ustc.edu.cn